Finite Element Analysis of Bilateral Double Rod Constructs in Thoracolumbar Fractures

Kemal PAKSOY[1], Idris AVCI[1], Ahmet Atilla ABDIOGLU[2], Salim SENTURK[1], Onur YAMAN[1]

[1]Memorial Hospital, Spine Center, Istanbul, Türkiye
[2]Fatih State Hospital, Department of Orthopaedics and Traumatology, Trabzon, Türkiye

Corresponding author: Idris AVCI ✉ mail.idrisavci@gmail.com

ABSTRACT

AIM: To evaluate bilateral double rod contructs in thoracolumbar fractures in a Finite Element model

MATERIAL and METHODS: A computed tomography of a 35-year old male have been chosen to create a vertebra model and 1/3 of the T12 was removed to create the burst fracture model. In model A, transpedicular polyaxial screws were inserted two levels above and two levels below the burst fracture. On each side the screws were connected with a single rod. In model B, the screws were connected with two rods on each side attached to two lateral connectors. A uniform 150 N axial load and 10 N/m torque was applied on the superior T10.

RESULTS: ROM and von Mises stress nephrograms revealed that the bilateral double-rod construct is being the most rigid and that the force on the pedicle screws were significantly lower compared to model A.

CONCLUSION: We believe that bilateral double-rod constructs for the stabilization of thoracolumbar fractures have a decreased load on pedicle screws and rods compared to the classic bilateral single rod stabilization system and can lower the risk of implant failure and the risk for secondary complications and revision surgery.

KEYWORDS: Thoracolumbar burst fractures, Implant failure, Screw breakage, Rod breakage, Finite element analysis

ABBREVIATIONS: CT: Computed tomography, **FEA:** Finite elemen analysis, **ROM:** Range of movement, **IF:** Implant failure, **TLF:** Thoracolumbar fracture

■ INTRODUCTION

Half of all vertebral fractures occur in the thoracolumbar junction, with burst fractures comprising two-thirds of these cases. Thoracolumbar burst fractures (TLF) are characterized by a compromised integrity of the anterior and middle vertebral columns, often resulting in instability and post-traumatic kyphosis. (19). Although its optimal treatment remains controversial, surgery is considered the gold standard for patients with instability and neurologic deficits, whether performed through a posterior, anterior or combined approach (4,20). In posterior stabilization surgery, long-segment instru-

mentation, involving fusion of more than two levels above and below the fracture, is the preferred option to achieve enhanced rigidity and correction of post-traumatic kyphosis (16). However, one of its drawbacks is the risk of implant failure (IF), such as screw and rod breakage. Till date, several biomechanical and clinical trials have been conducted to investigate TLF surgery (12). Some studies have explored the use of classic bilateral single-rod fixation systems, with or without interbody fusion, for TLF. However, no finite element analyses (FEA) have been conducted on long-segment stabilization of TLF surgery with bilateral double-rod systems. Therefore, this study developed an FEA model of TLF with long-segment

Kemal PAKSOY (ID) : 0000-0002-7677-7356
Idris AVCI (ID) : 0000-0002-0378-9356
Ahmet Atilla ABDIOĞLU (ID) : 0000-0002-0206-8135
Salim SENTURK (ID) : 0000-0003-0524-9537
Onur YAMAN (ID) : 0000-0002-2038-1643

stabilization and bilateral double-rod fixation and assessed its biomechanical characteristics in comparison to bilateral single-rod fixation. Moreover, bilateral double-rod constructs are hypothesized to exert less stress on pedicle screws and rods, potentially reducing the risk of IF.

■ MATERIAL and METHODS

The ethical committee's approval was obtained in accordance with the Helsinki Declaration (Memorial Bahcelievler; approval number: 72, date: 05.01.2023). Written consent was obtained from a healthy individual for the creation of a vertebra model.

Creating the Finite Element model

A healthy 35-years old male with no confirmed history of spinal trauma or lesions, was selected to create the vertebra model for FEA. A computed tomography (CT) scan of the T9-L3 region was performed using a Siemens SOMATOM Definition Flash device (*Siemens AG, Erlangen, Germany*), capturing 1 mm thick image slices in the Digital Imaging and Communications in Medicine (DICOM) format.

A three-dimensional homogenous model was generated using Rhinoceros v. 4.0 (*Robert McNeel & Associates, Seattle, WA, USA*) and VRMesh Studio (*Virtual Grid Inc., Bellevue City, WA, USA*) software. Subsequently, the models were imported into the Algor Fempro (*ALGOR Inc., Pittsburgh, PA, USA*) application for analysis. An 8-knot type element was utilized for meshing the models, which were then converted into brick and tetrahedral solid elements. The resulting models in .stl format were subsequently imported back into Rhinoceros software. Since the structure of the intervertebral disc could not be delineated using the CT images, its geometric and anatomical features were reconstructed based on previously published FEA models of the spine (9). In Rhinoceros, the continuity between the disc and the vertebral endplates was designed using the Boolean method, while dimensional and topographic characteristics were added in VRMesh. We employed mesh surface modeling (Mesh First Approach) to obtain highly detailed and realistic organic 3D models that cannot be achieved through parametric surface modeling.

The final model was integrated into the x, y, z-coordinates within Rhinoceros, completing the model creation process. The entire FEA analysis was conducted on a computer running Microsoft Windows 7 Ultimate, equipped with an Intel Xeon R 3.5 GHz processor, 14 GB of RAM, and a 500 GB storage capacity.

Creating the thoracolumbar burst fracture model

To create the TLF model, the inferior one-third of the T12 vertebra and the intervertebral disc between T12-L1 were removed using VRMesh, following the methodology established in previous publications on TLF FEA models (5). Subsequently, the final model was imported into Algor Fempro and subdivided into planar-braided structures.

Fixation models

To simulate the fixation of TLF, two different models were used. In Model A, transpedicular polyaxial screws were insert-

ed two levels above and two levels below the burst fracture. On each side, the screws were connected with a single rod. In Model B, the screws were linked with two rods on each side, attached to two lateral connector (domino) devices between T11-T12 and L1-L2. In both models, each screw had a width and length of 6.5 mm and 45 mm, repectively (Figure 1). The physical characteristics, including elasticity model and Poisson's ratio, are detailed in Table I. To validate the model's rationale, a torque of 10 N/m and a compression force of 150 N were applied to the superior T10 vertebra. The range of movement (ROM) under this load, in the form of flexion, extension, lateral bending, and rotation, was simulated and compared to two other biomechanical models by Pflugmacher (14) and Li (11) (Table II).

Boundary and loading Conditions

Latitude degrees below the L2 vertebra were restricted. A combination of a 150 N preload and a 10 N/m pure moment force was applied to the superior T10 vertebra, simulating flexion, extension, lateral bending, and rotational movements.

Analytic criteria

The ROM within the region spanning from T10 to L2 and the stress experienced by the pedicle screws and rods in both Model A and B, were analyzed using six distinct von Mises tension and stress criteria: flexion, extension, left lateral bending, right lateral bending, left rotation, and right rotation.

■ RESULTS

Range of motion

A uniform axial load of 150 N and a torque of 10 N/m were applied to the superior T10 vertebra, and the range of motion (ROM) for each side was recorded. In Model A, the results were as follows: 1.5° for flexion, 1.1° for extension, 1.9° for left lateral bending, 1.8° for right lateral bending, 1.6° for left axial rotation, and 1.6° for right axial rotation. In Model B, the ROM values were 1.3° for flexion, 1.0° for extension, 1.8° for left lateral bending, 1.8° for right lateral bending, 1.7° for left axial rotation, and 1.6° for right axial rotation.
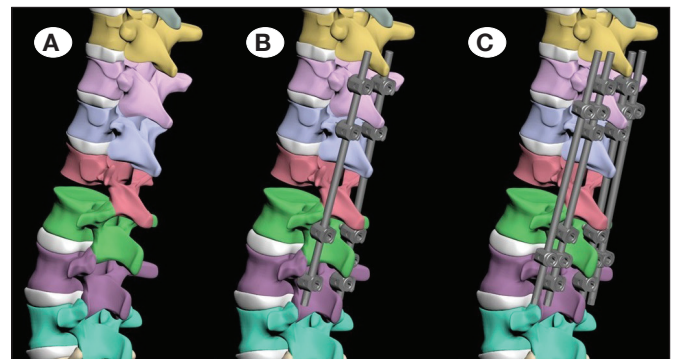

Figure 1: A) 3D- thoracolumbar burst fracture model; **B)** Burst fracture model with bilateral single rod fixation (model A); **C)** Burst fracture model with bilateral double-rod fixation model (model B).

Table I: Material Properties in the Present Finite Element Model

Component	Young's modulus (MPa)	Poisson's ratio	Cross section (mm²)
Vertebra			
Cortical bone	12000	0.30	
Cancellous bone	100	0.20	
End plate	1000	0.4	
Intervertebral disc			
Annulus fibrosus	450	0.45	
Nucleus pulposus	0.2	0.49	
Ligaments			
Anterior longitudinal ligaments	20	0.40	63.7
Posterior longitudinal ligaments	20	0.30	20
Supraspinous and interspinous ligaments	10	0.30	40
Ligamentum flavum	15	0.30	40
Intertransverse ligament	10	0.30	40
Capsular ligament	8	0.30	30
Pedicle screw, lateral connector and rods	110000	0.30	

Table II: Comparision of Range of Movement of Our Results and Plugmacher and Li's Findings

Motion	Model A	Model B	Pflugmacher	Li
Flexion	4.5	4.4	5.3	4.6
Extension	4.7	4.3	5.7	4.5
Left lateral bending	4.0	4.1	4.3	4.6
Right lateral bending	4.0	4.2	4.3	4.8
Left axial rotation	2.9	2.1	2.1	3.2
Right axial rotation	2.9	2.1	2.1	3.2

Maximum von Mises tension on pedicle screws and rods

In the bilateral single-rod model (Model A), the von Mises tension on the pedicle screws was measured as follows: 87.9 MPa in flexion, 94.7 MPa in extension, 110.7 MPa in left lateral bending, 112.3 MPa in right lateral bending, 37.9 MPa in left rotation, and 36.3 MPa in right rotation.

In the bilateral double-rod construct (Model B), the tension on the pedicle screws was as follows: 38.7 MPa in flexion, 46.7 MPa in extension, 61.8 MPa in left lateral bending, 64.3 MPa in right lateral bending, 32.9 MPa in left rotation, and 31.2 MPa in right rotation.

Regarding Model A, the tension on the rods was calculated as 177.2 MPa in flexion, 195.7 MPa in extension, 203.3 MPa in left lateral bending, 197.7 MPa in right lateral bending, 147.4 MPa in left rotation, and 155.6 MPa in right rotation. In Model B, the results were as follows: 133.5 MPa, 144.6 MPa, 138.6 MPa, 137.2 MPa, 132.3 MPa, and 135.3 MPa, respectively

Von Mises stress distribution nephogram on pedicle screws and rods

The von Mises tension distribution reveals that in both Model A and B, stress is exerted on both the rods and screws during flexion, extension, axial rotation, and lateral bending movements. Numerical values were significantly lower in Model B (Figure 2A-D). Stress during flexion and extension is primarily concentrated on the rods (Figure 2A, B). During lateral bending, the stress on the rods is most pronounced (Figure 2D). Higher tension on screws is observed in Model A, while the rods in Model A experience more tension than in the bilateral double-rod construct. The overall stress distribution
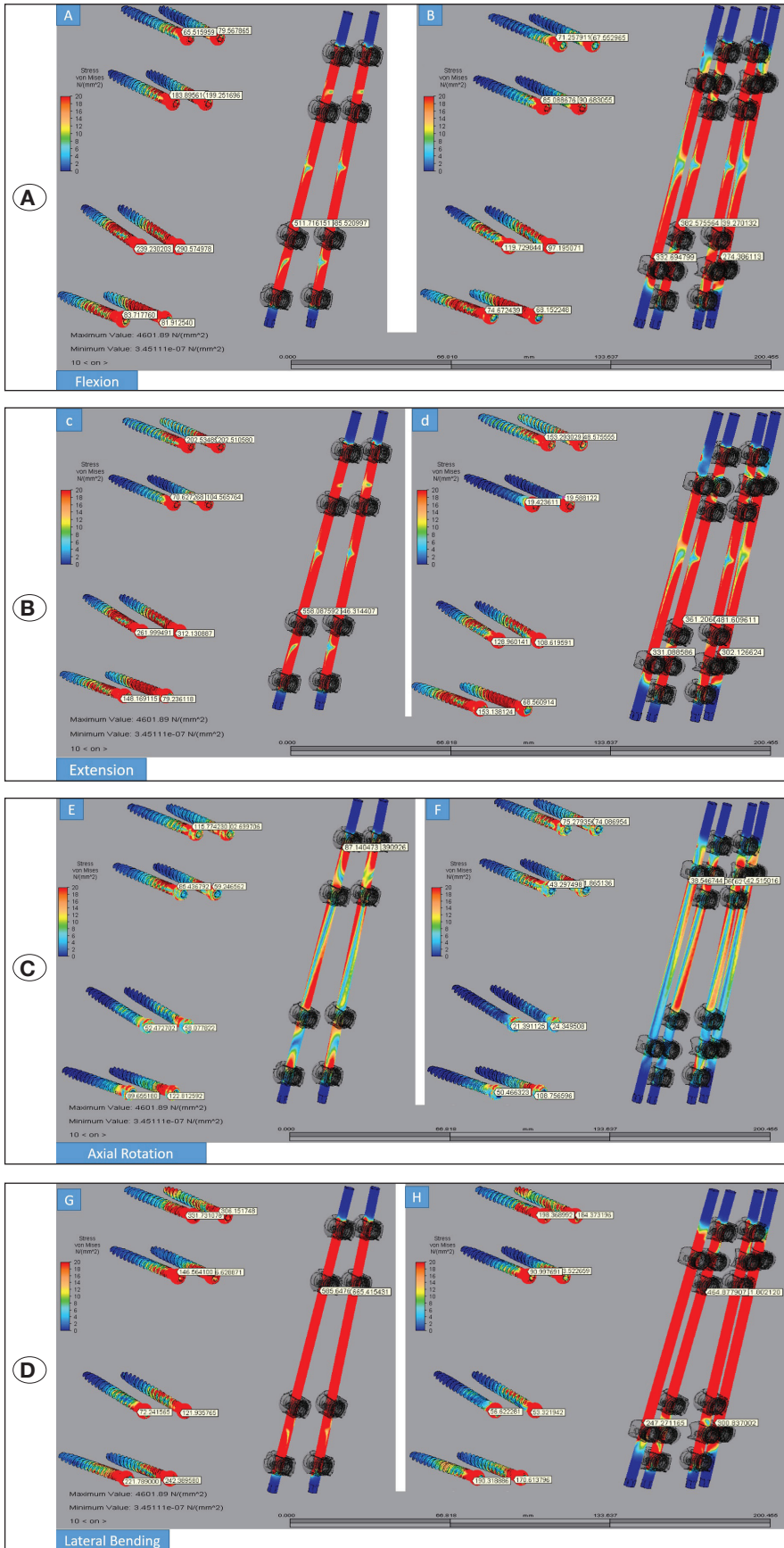
Figure 2: A) von Mises stress nephogram during flexion. In both simulations stress is distributed towards the rods and screws. Numerical values are lower in model B. **B)** von Mises stress nephogram during extension. In both simulations stress is distributed towards the rods and screws. Numerical values are lower in model B. **C)** von Mises stress nephogram during axial rotation. In both simulations stress is distributed towards the rods and screws. Numerical values are lower in model B. **D)** von Mises stress nephogram during lateral bending. In both simulations stress is distributed towards the rods and screws. Numerical values are lower in model B.

indicates that stress on the screws and rods during all ROM simulations is significantly lower in Model B (Figure 3).

■ DISCUSSION

The thoracolumbar junction, where the more rigid thoracic vertebral region transitions to the more mobile lumbar region, is inherently susceptible to increased axial loads and fractures (7). In cases of thoracolumbar burst fractures (TLF), early stabilization is considered the gold standard when instability and neurologic deficits are present (15). Surgical approaches for these fractures encompass posterior, anterior, or combined

methods (19). In posterior approaches, some authors advocate for short-segment stabilization, involving fixation of only one vertebra above and one vertebra below the fracture. This approach is favored for its benefits, including reduced blood loss, shorter surgery time, and fewer implantation materials. Conversely, other authors recommend long-segment stabilization for improved rigidity and a better chance of correcting post-traumatic kyphosis (17). One of the most common complications associated with posterior stabilization of TLF is implant failure (IF), often resulting from bending or breakage of screws and rods due to increased physical stresses during flexion, extension, bending, or rotational maneuvers (13). Literature reports indicate an incidence ranging from 20% to 39% (10,17,18). In a 2014 case series by Eldin and Ali (8), which included 200 patients with IF, screw breakage was reported as the most common type of implant failure, followed by rod fracture, rod loosening, screw loosening, and combinations of rod and screw loosening. Patients with IF typically experience moderate to severe back pain, and the risk of kyphosis and the need for revision surgery increase when the implanted construct is compromised (3). To address these complications, numerous biomechanical and clinical trials have been conducted, yet the incidence of IF remains high. In classic posterior stabilization of TLF, fixation is primarily achieved using single rod constructs bilaterally attached to pedicle screws. Some authors suggest that, especially in cas-

Table III: Evaluation of ROM between Model A and Model B

	Model A	Model B
Flexion	1.5	1.3
Extension	1.1	1.0
Left Lateral Bending	1.9	1.8
Right Lateral Bending	1.8	1.8
Left Rotation	1.6	1.7
Right Rotation	1.6	1.6

Table IV: von Mises Tension on Pedicle Screws and Rods

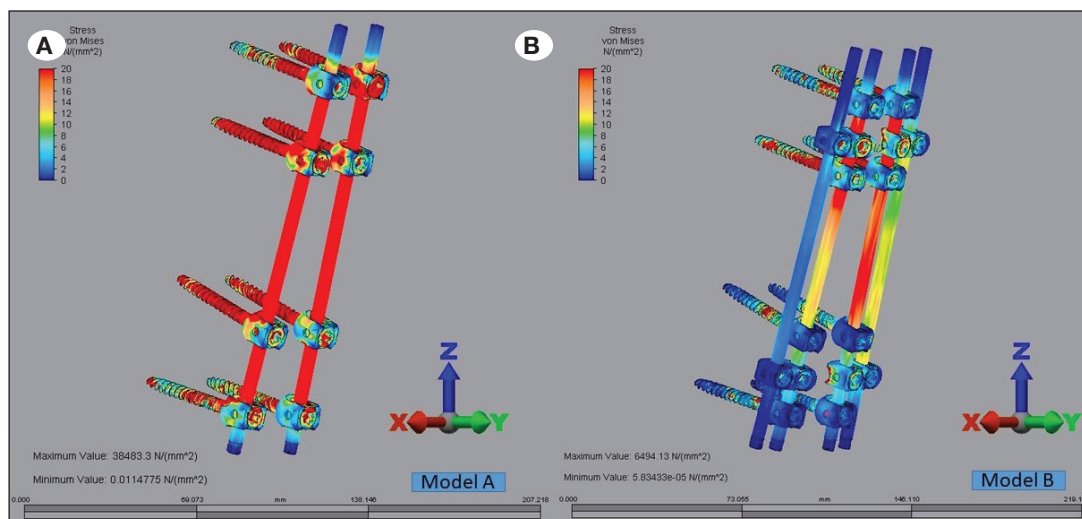| ROM	Model A (screw)	Model B (screw)	Model A (rod)	Model B (rod)
Flexion	87.9 MPa	38.7 MPa	177.2 MPa	133.5 MPa
Extension	94.7 MPa	46.7 MPa	195.7 MPa	144.6 MPa
Left lateral bending	110.7 MPa	61.8 MPa	203.3 MPa	138.6 MPa
Right lateral bending	112.3 MPa	64.3 MPa	197.7 MPa	137.2 MPa
Left rotation	37.9 MPa	32.9 MPa	147.4 MPa	132.3 MPa
Right rotation	36.3 MPa	31.2 MPa	155.6 MPa	135.3 MPa

Figure 3: Overall von Mises stress nephogram. **A)** Model A, increased stress on rods and screws (red) **B)** Model B, moderate stress on rods and screws (blue).

es of osteoporosis, bone-cement-injected fenestrated pedicle screws may enhance stability (2). Additionally, instrumentation of the fractured level, provided the pedicles are intact, may improve the stability of posterior fixation (1). In posterior fusion surgery, the primary physical loads are borne by the instrumented pedicle screws. When the implanted materials fail to fuse with the vertebra, the force on the screws, particularly at the screw neck, increases, potentially leading to breakage. If the screws withstand the pressure, the rods, being the next vulnerable point, may bend and break. In rare cases, a combination of both scenarios can occur (6). In our model, we hypothesized that double rods could enhance construct stability. In 2004, Pflugmacher et al. analyzed range of motion (ROM) in patients who underwent posterior fusion surgery with expandable and non-expandable cages (14). Li et al. evaluated ROM in patients who underwent short-segment stabilization at the thoracolumbar junction (11). Compared to both studies, our results indicate that in both Model A and B, ROM during flexion, extension, bending, and rotation decreased. Notably, Model B exhibited a slightly greater decrease in ROM, suggesting that the bilateral double-rod construct is the most rigid among all constructs compared to previous biomechanical analyses.

Our von Mises stress evaluation of the pedicle screws in FEA revealed that in the double-rod construct model (Model B), the forces on the pedicle screws were significantly lower than in the bilateral single-rod model (Model A), suggesting a reduced risk of pedicle screw loosening or breakage. Moreover, the forces applied to the rods were notably lower in Model B, indicating a lower probability of rod damage. There are multiple reasons for the preference for FEA over mechanical testing. In today's context, many phenomena have been succesfully simulated in the computer environment. Virtually everything can be adapted and subjected to analysis within the computer technical realm. A wealth of data can be acquired more rapidly in the digital environment than in reality. Any object consist of an infinite number of elements, but we divide these objects into a finite number of parts within the digital surrounding for computation purposes. This yields mathematical data. When we subject this obtained data to analysis, we can select any specific region and get the highest stress data from a particular point. In the event of revisions, we can swiftly subject the same model to analysis and obtain results. Through the model, we can visualize stress distribution, identify areas of stress concentration and observe a homogenized stress map. Nonetheless, there are limitations to our study. Primarily, we created a single spine model based on a healthy male individual. To generalize our findings, a diverse sample should be considered, including individuals of varying ages and genders. Additionally, our model does not account for the influence of paravertebral muscles and ligaments, which play a significant role in spinal stability. These factors should be incorporated into future investigations.

■ **CONCLUSION**

Our FEA model demonstrated that bilateral double-rod constructs used for stabilizing thoracolumbar fractures impose reduced loads on pedicle screws and rods compared to the traditional bilateral single-rod stabilization system. This suggests that they may mitigate the risk of implant failure and lower the likelihood of secondary complications, potentially reducing the need for revision surgery.

■ **REFERENCES**

1. Abousayed M, Boktor JG, Sultan AM, Koptan W, El-Miligui Y: Augmentation of fenestrated pedicle screws with osteoporotic spine. J Craniovertebr Junction Spine 9:20-25, 2018. https://doi.org/10.4103/jcvjs.JCVJS_14_18

2. Altay M, Ozkurt B, Aktekin CN, Ozturk AM, Dogan O, Tabak AY: Treatment of unstable thoracolumbar junction burst fractures with short- or long-segment posterior fixation in magerl type a fractures. Eur Spine J 16:1145-1155, 2007. https://doi.org/10.1007/s00586-007-0310-5

3. Alvine GF, Swain JM, Asher MA, Burton DC: Treatment of thoracolumbar burst fractures with variable screw placement or Isola instrumentation and arthrodesis: Case series and literature review. J Spinal Disord Tec 17:251-264, 2004. https://doi.org/10.1097/01.bsd.0000095827.98982.88

4. Aly TA: Short segment versus long segment pedicle screws fixation in management of thoracolumbar burst fractures: Meta-analysis. Asian Spine J 11:150-160, 2017. https://doi.org/10.4184/asj.2017.11.1.150

5. Basaran R, Efendioglu M, Kaksi M, Celik T, Mutlu I, Ucar M: Finite element analysis of short- versus long-segment posterior fixation for thoracolumbar burst fracture. World Neurosurg 128:e1109-e1117, 2019. https://doi.org/10.1016/j.wneu.2019.05.077

6. Burval DJ, McLain RF, Milks R, Inceoglu S: Primary pedicle screw augmentation in osteoporotic lumbar vertebrae: Biomechanical analysis of pedicle fixation strength. Spine 32:1077-1083, 2007. https://doi.org/10.1097/01.brs.0000261566.38422.40

7. Du Plessis A, Van Schoor A, Wessels Q, Murphy P, Van Schowenburg F, Ihuhua P, Kehrmann J, Scholtz M, Natalie Keough N: Vertebrae at the thoracolumbar junction: A quantitative assessment using CT scans. J Anat 240:1179-1186, 2022. https://doi.org/10.1111/joa.13619

8. Eldin MMM, Ali AMA: Lumbar transpedicular implant failure: A clinical and surgical challenge and its radiological assesment. Asian Spine J 8:281-297, 2014. https://doi.org/10.4184/asj.2014.8.3.281

9. Goto K, Tajima N, Chosa E, Totoribe K, Kuroki H: Mechanical analysis of the lumbar vertebrae in a three-dimensional finite element method model in which intradiscal pressure in the nucleus pulposus was used to establish the model. J Orthop Sci 7:243-246, 2002. https://doi.org/10.1007/s007760200040

10. Heary RF, Kumar S: Decision-making in burst fractures of the thoracolumbar and lumbar spine. Indian J Orthop 41:268-276, 2007. https://doi.org/10.4103/0019-5413.36986

11. Li C, Zhou Y, Wang H, Liu J, Xiang L: Treatment of unstable thoracolumbar fractures through short segment pedicle screw fixation techniques using pedicle screw fixation at the level of the fracture: A finite element analysis. PLos One 9:e99156, 2014. https://doi.org/10.1371/journal.pone.0099156

12. Norton RP, Milne EL, Kaimrajh DN, Eismont FJ, Latta LL, Williams SK: Biomechanical analysis of four- versus six-screw constructs for short-segment pedicle screw and rod instrumentation of unstable thoracolumbar fractures. Spine J 14:1734-1739, 2014. https://doi.org/10.1016/j.spinee.2014.01.035

13. Park WM, Choi DK, Kim K, Kim YJ, Kim YH: Biomechanical effects of fusion levels on the risk of proximal junctional failure and kyphosis in lumbar spinal fusion surgery. Clin Biomech 30:1162-1169, 2015. https://doi.org/10.1016/j.clinbiomech.2015.08.009

14. Pflugmacher R, Schleicher P, Schaefer J, Scholz M, Ludwig K: Biomechanical comparison of expandable cages for vertebral body replacement in the thoracolumbar spine. Spine 29:1413-1419, 2004. https://doi.org/10.1097/01.BRS.0000129895.90939.1E

15. Prajapati HP, Kumar R: Thoracolumbar fracture classification: Evolution, merits, demerits, updates, and concepts of stability. Br J Neurosurg 35:92-97, 2021. https://doi.org/10.1080/02688697.2020.1777256

16. Rispoli R, Abousayed M, Hamed AA, Cappelletto B: Long versus short segment with intermediate screw fixation for burst fractures of thoracolumbar junction: Radiological and clinical results. J Neurosurg Sci 2022 (Online ahead of print). https://doi.org/10.23736/S0390-5616.22.05794-0

17. Sapkas G, Kateros K, Papadakis S, Brilakis E, Macheras G, Katonis P: Treatment of unstable thoracolumbar burst fractures by indirect reduction and posterior stabilization: Short-segment versus long-segment stabilization. Open Orthop J 15:7-13, 2010. https://doi.org/10.2174/1874325001004010007

18. Yu SW, Fang KF, Tseng IC, Chiu YL, Chen YJ, Chen WJ: Surgical outcomes of short-segment fixation for thoracolumbar fracture dislocation. Chang Gung Med J 25:253-259, 2002

19. Wood KB, Li W, Lebl DR, Ploumis A: Management of thoracolumbar fractures. Spine J 14:145-164, 2014. https://doi.org/10.1016/j.spinee.2012.10.041

20. Zhu Q, Shi F, Cai W, Bai J, Fan J, Yang H: Comparison of anterior versus posterior approach in the treatment of thoracolumbar fractures: A systematic review. Int Surg 100:1124-1133, 2015. https://doi.org/10.9738/INTSURG-D-14-00135.1